Nonsimilar solution of an unsteady mixed convection flow on a moving slender cylinder

D. Anilkumar*, S. Roy

Department of Mathematics, Indian Institute of Technology, Chennai, 600036, India

Abstract

A general analysis has been developed to study the flow and heat transfer characteristics of an unsteady laminar mixed convection on a continuously moving vertical slender cylinder. The governing boundary layer equations along with the boundary conditions are first cast into a dimensionless form by a nonsimilar transformation and the resulting system of nonlinear coupled partial differential equations is then solved by an implicit finite difference scheme in combination with the quasilinearization technique.

Keywords: Mixed convection; Vertical slender cylinder; Quasilinearization; Nonsimilar solution; Boundary layer; Heat transfer

1. Introduction

Unsteady mixed convection flows do not necessarily admit similarity solutions in many practical situations. Flows over cylinder are usually considered to be two dimensional as long as the body radius is large compared to the boundary layer thickness. On the other hand, for a slender cylinder, the radius of the cylinder may be of the same order as that of the boundary layer thickness. Therefore, the flow may be considered as axisymmetric instead of two dimensional. Mixed convection flow over a slender vertical cylinder due to the thermal diffusion has been considered by Chen et al. [1] and Mucoglu et al. [2] for the constant wall temperature and constant heat flux conditions, respectively. Subsequently, Bui et al. [3], Wang et al. [4] and, most recently, Takhar et al. [5] have solved this problem using an implicit finite difference scheme. All the above studies pertain to steady flows. In many practical problems, the flow could be unsteady. Therefore, as a step towards the eventual development on unsteady mixed convection flows, it is interesting as well as useful to investigate the combined effects of transverse curvature, viscous dissipation and thermal diffusion on a continuously moving vertical slender cylinder.

* Corresponding author. Tel.: +91 (44) 2257 8492; Fax: +91 (44) 2257 0593; E-mail: anil@iitm.ac.in

Computational Fluid and Solid Mechanics 2005
K.J. Bathe (Editor)

2. Analysis

We consider the unsteady laminar mixed convection flow along a heated vertical slender cylinder. The unsteadiness in the flow field is introduced by the cylinder velocity and free stream velocity which vary with time. The flow is taken to be axisymmetric and the Boussinesq approximation is invoked for the fluid properties to relate density changes to temperature changes. Under the above assumptions, the governing boundary layer equations can be expressed as [5,6,7]

$$\frac{\partial(ru)}{\partial x}+\frac{\partial(rv)}{\partial r}=0 \tag{1}$$

$$\frac{\partial u}{\partial t}+u\frac{\partial u}{\partial x}+v\frac{\partial u}{\partial r}=\frac{\partial u_e}{\partial t}+(\nu/r)\frac{\partial}{\partial r}\left(r\frac{\partial u}{\partial r}\right)+g\beta(T-T_\infty) \tag{2}$$

$$\frac{\partial T}{\partial t}+u\frac{\partial T}{\partial x}+v\frac{\partial T}{\partial r}=\frac{\nu}{Pr}\frac{1}{r}\frac{\partial}{\partial r}\left(r\frac{\partial T}{\partial r}\right)+\frac{\mu}{\rho c_p}\left(\frac{\partial u}{\partial r}\right)^2 \tag{3}$$

The initial conditions are

$$u(0,x,r)=u_i(x,r),\quad v(0,x,r)=v_i(x,r),$$
$$T(0,x,r)=T_i(x,r) \tag{4}$$

and the boundary conditions are given by

$$u(t,x,R)=u_w(t)=u_{w,0}\phi(t*),\quad v(t,x,R)=0,$$

$$T(t,x,R)=T_w,\quad u(t,x,\infty)=u_e(t)=u_\infty\phi(t*),$$
$$T(t,x,\infty)=T_\infty \tag{5}$$

Here x and r are axial and radial co-ordinates and u, v are the velocity components in the axial and radial directions, respectively; t is the time; g is the acceleration due to gravity; α and ν are thermal diffusivity and kinematic viscosity, respectively; K is the thermal conductivity; T is the temperature in the boundary layer; and β is the volumetric co-efficient of thermal expansion.

Applying the following transformations:

$$\xi=\left(\frac{4}{R}\right)\left(\frac{\nu x}{u_\infty}\right)^{\frac{1}{2}},\quad \eta=\left(\frac{\nu x}{u_\infty}\right)^{-\frac{1}{2}}\left[\frac{r^2-R^2}{4R}\right],\quad t^*=\frac{\nu}{R^2}t,$$
$$\frac{r^2}{R^2}=[1+\xi\eta],\quad \psi(x,r,t)=R(\nu u_\infty x)^{\frac{1}{2}}\phi(t^*)f(\xi,\eta,t^*),$$
$$u=\frac{1}{2}u_\infty\phi f_n,\quad v=\frac{1}{2r}R\phi\left(\frac{\nu u_\infty}{x}\right)^{\frac{1}{2}}\left(\eta f_\eta-f-\xi\frac{\partial f}{\partial\xi}\right),$$
$$G(\xi,\eta,t^*)=\frac{T-T_\infty}{T_w-T_\infty},\quad Ec=\frac{{u_\infty}^2}{4c_p(T_w-T_\infty)},\quad \lambda=\frac{Gr_x}{Re_x^2},$$
$$Pr=\frac{\nu}{\alpha},\quad Gr_x=g\beta x^3(T_w-T_\infty)/\nu^2,\quad Re_x=\frac{u_\infty x}{\nu} \tag{6}$$

to Eqs. (1)–(3), we find that Eq. (1) is identically satisfied, and Eqs. (2)–(3) reduce to

$$[(1+\xi\eta)F_\eta]_\eta+\phi fF_\eta+8\lambda\phi^{-1}G+\left(\frac{\xi^2}{4}\right)[\phi^{-1}\phi_{t^*}(2-F)-$$
$$F_{t^*}]=\phi\xi[FF_\xi-F_\eta f_\xi] \tag{7}$$
$$Pr^{-1}[(1+\xi\eta)G_\eta]_\eta+\phi fG_\eta+Ec(1+\xi\eta)\phi^2F_\eta^2-\frac{\xi^2}{4}G_{t^*}=$$
$$\phi\xi[FG_\xi-G_\eta f_\xi] \tag{8}$$

The boundary conditions for these equations are expressed by

$$F(\xi,0,t^*)=\alpha,\quad G(\xi,0,t^*)=1\quad \text{for}\quad 0\le t^*,\xi\le 1$$
$$F(\xi,\infty,t^*)=2,\quad G(\xi,\infty,t^*)=0\quad \text{for}\quad 0\le t^*,\xi\le 1 \tag{9}$$

where $\alpha=2\left(\frac{u_w}{u_e}\right)$ and $f(\xi,\eta,t^*)=\int_0^\eta F dx$.

Here η is the similarity variable; ξ is the transverse curvature; f and f_η are the dimensionless stream functions and velocity components, respectively; G and t^* are the dimensionless temperature and time respectively; Re_x is the Reynolds number; Pr is the Prandtl number; Gr_x is the Grashof number, λ is the buoyancy parameter; $\phi(t^*)$ is the function of t^* with first order continuous derivative; c_p is the specific heat at constant pressure; and ϵ is constant.

The quantities of physical interest are as follows [6,7]: The local surface skin friction coefficient given by

$$C_f=\frac{2\tau_w}{\rho u_\infty^2}=2^{-1}Re_x^{-\frac{1}{2}}\phi(t^*)(F_\eta)_w$$

Thus,

$$Re_x^{\frac{1}{2}}C_f=2^{-1}\phi(t^*)(F_\eta)_w$$

The local Nusselt number can be expressed as

$$Re_x^{-\frac{1}{2}}Nu=-2^{-1}(G_\eta)_w \tag{10}$$

where

$$Nu=-\frac{\left[x\left(\frac{\partial T}{\partial r}\right)\right]_w}{T_w-T_\infty}$$

3. Method of solution

The set of dimensionless equations (7)–(8) under the boundary conditions (9) with the initial conditions obtained from the corresponding steady state equations has been solved numerically using an implicit finite difference scheme in combination with the quasilinearization technique. Since the method is described by Inouye et al. [8], its detailed description is not presented here for the sake of brevity. In brief, the non-linear coupled partial differential equations were replaced by an iterative sequence of linear equations following the quasilinearization technique. The resulting sequence of linear partial differential equations were expressed in difference form using the central difference scheme in the η-direction and the backward difference scheme in the ξ- and t^*-directions. In each iteration step, the equations were then reduced to a system of linear algebraic equations with a block tri-diagonal structure, which is solved by using Varga's algorithm [9]. A convergence criteria based on the relative difference between the current and previous iteration values are employed. When the difference reaches less than 10^{-4}, the solution is assumed to have converged and the iterative process is terminated.

4. Results and discussion

The computations have been carried out for various values of Pr ($0.7\le Pr\le 7.0$), λ ($0\le\lambda\le 3$), α ($0\le\alpha\le 2$) and Ec ($0\le Ec\le 0.3$). The edge of the boundary layer η_∞ is taken between 3 and 5 depending on the values of parameters. The results have been obtained for both accelerating ($\phi(t^*)=1+\epsilon t^{*2}$, $\epsilon>0$, $0\le t^*\le 1$) and decelerating ($\phi(t^*)=1+\epsilon t^{*2}$, $\epsilon<0$, $0\le t^*\le 1$) free stream velocities of the fluid. In order to validate our method, we have compared steady state results of skin-friction and heat transfer coefficients ($F_\eta(0,0)$, $G_\eta(0,0)$,)

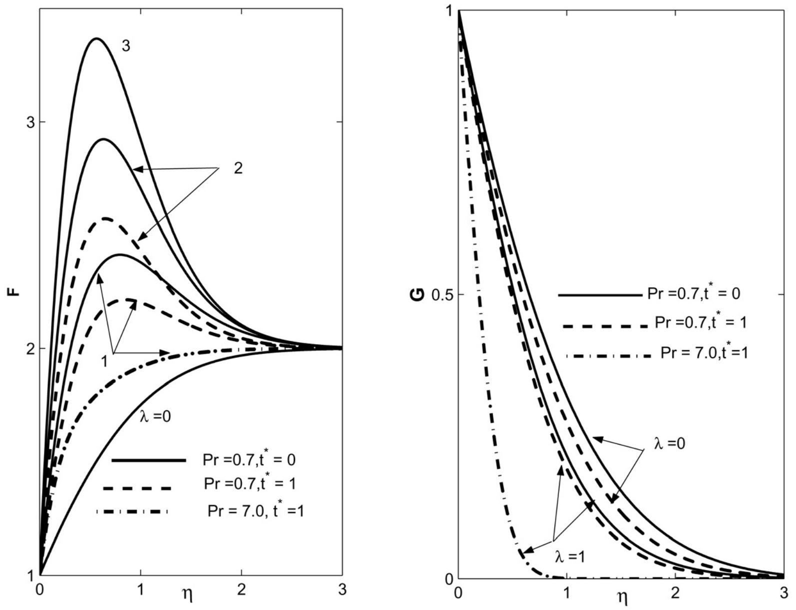

Fig. 1. Effects of λ and Pr on F and G for $\phi(t^*) = 1 + \epsilon t^2$, $\epsilon = 0.5$ when $Ec = 0.1$, $\alpha = 1$, $\xi = 0.5$.

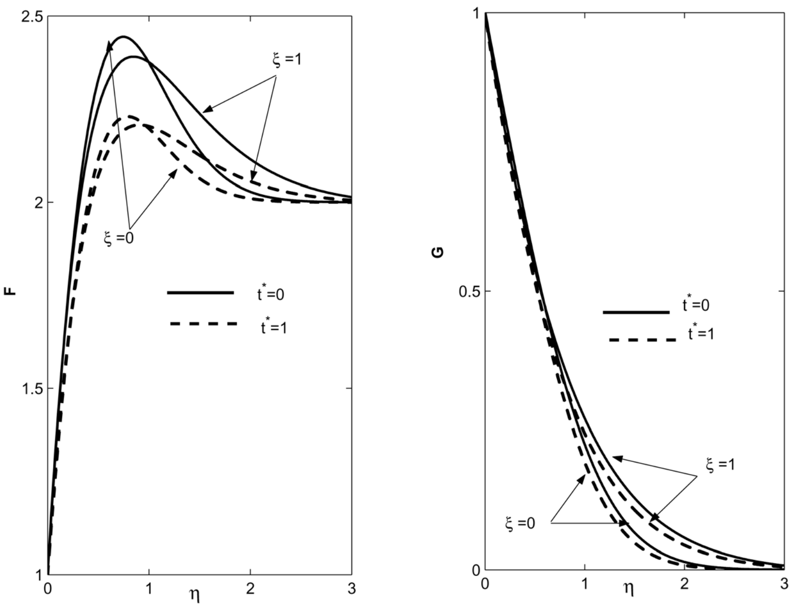

Fig. 2. Effect of ξ on F and G for $\phi(t^*) = 1 + \epsilon t^2$, $\epsilon = 0.5$ when $\lambda = 1$, $Pr = 0.7$, $Ec = 0.1$, $\alpha = 1$.

with those of Chen et al. [1] and Takhar et al. [5], and the results are found to be in excellent agreement.

The effects of the surface curvature parameter ξ (or the axial distance) and the buoyancy parameter λ on the velocity and temperature profiles (F, G) for accelerating flow $\phi(t^*) = 1 + \epsilon t^{*2}$, $\epsilon = 0.5$, when $\alpha = 1$, $Ec = 0.1$, $Pr = 0.7$ and 7.0, are displayed in Figs. 1–2. Also, the effects of ξ and λ on the skin friction and heat transfer coefficients are presented in Fig. 3. The action of the buoyancy force shows the overshoot in the velocity profiles (F) near the wall for lower Prandtl number ($Pr = 0.7$) but for higher Prandtl number ($Pr = 7.0$) the velocity overshoot in F is not observed as shown in Fig. 1. The reason is that the buoyancy force (λ) effect is

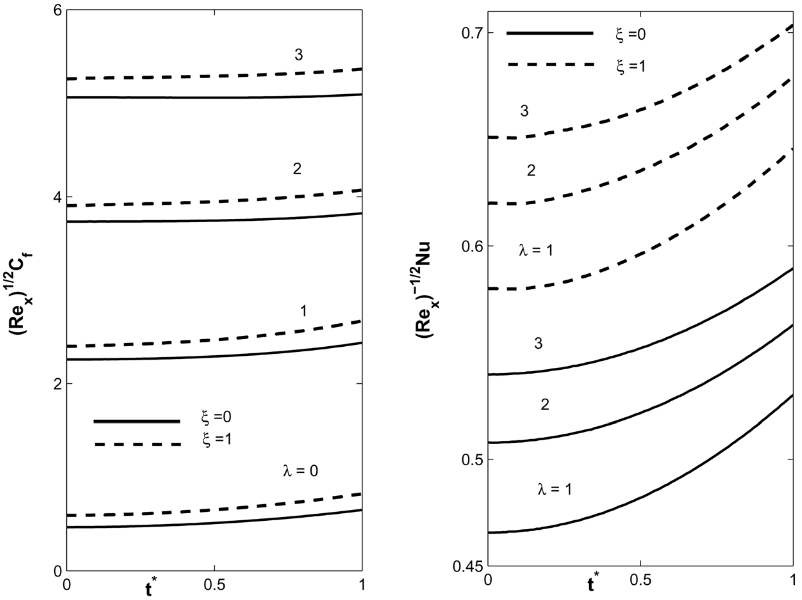

Fig. 3. Effects of λ and ξ on $Re_x^{1/2}C_f$ and $Re_x^{-1/2}Nu$ for $\phi(t^*) = 1 + \epsilon t^2$, $\epsilon = 0.5$ when $Pr = 0.7$, $Ec = 0.1$, $\alpha = 1$.

larger in a low Prandtl number fluid ($Pr = 0.7$, air) due to the lower viscosity of the fluid, which enhances the velocity as the assisting buoyancy force acts like a favorable pressure gradient and the velocity overshoot occurs. For a higher Prandtl number fluid ($Pr = 7.0$, water) the velocity overshoot is not present because a higher Prandtl number fluid implies a more viscous fluid, which makes it less sensitive to the buoyancy parameter λ. The effect of λ is comparatively less on the temperature (G), as shown in Fig. 1. Due to the increase in the surface curvature parameter ξ, the steepness in the velocity and temperature profiles (F, G) near the wall increases, but the magnitude of the velocity overshoot is slightly decreased, as can be seen in Fig. 2. Further from Fig. 3, it is observed that the skin friction and heat transfer coefficients ($\mathrm{Re}_x^{1/2}\mathrm{C_f}, \mathrm{Re}_x^{-1/2}\mathrm{Nu}$) increase with the increase of the buoyancy parameter λ. The physical reason is that the positive buoyancy force ($\lambda > 0$) implies a favorable pressure gradient and therefore the fluid gets accelerated, which results in thinner momentum and thermal boundary layers. Consequently, the local skin friction and Nusselt number are also increased at any time (t^*), as shown in Fig. 3.

Figures 4 and 5 display the effects of Pr and Ec for accelerating and decelerating freestream flows on the local skin friction and heat transfer coefficients ($\mathrm{Re}_x^{1/2}\mathrm{C_f}, \mathrm{Re}_x^{-1/2}\mathrm{Nu}$), where $\alpha = 1.0$ and $\lambda = 1.0$. It is found from Fig. 4 that the skin friction coefficient decreases with the increase in the Prandtl number. Because the higher Prandtl number means that the fluid is more viscous, this increases the boundary layer thickness and consequently reduces the shear stress. On the other hand, Fig. 5 reveals that the surface heat transfer rate increases significantly with Pr, as the higher Pr fluid has a lower thermal conductivity, which results in a thinner thermal boundary layer and hence a higher heat transfer rate at the wall. It is observed from Fig. 5 that, due to increase of the viscous dissipation parameter Ec, $\mathrm{Re}_x^{1/2}\mathrm{C_f}$ increases but $\mathrm{Re}_x^{-1/2}\mathrm{Nu}$ decreases, with a more pronounced effect on the heat transfer coefficient ($\mathrm{Re}_x^{-1/2}\mathrm{Nu}$). In particular, it is found for an accelerating flow ($\epsilon = 0.5$) that the percentage decrease of $\mathrm{Re}_x^{-1/2}\mathrm{Nu}$ for an increase in Ec from 0 to 0.2 at $t^* = 1.0$ is 100%, as compared to 10% of $\mathrm{Re}_x^{1/2}\mathrm{C_f}$ for the same data. This behavior is in support of the common fact that the viscous dissipation affects the thermal boundary layer more than the momentum boundary layer. In the case of an accelerating flow, Fig. 4 shows that both skin friction coefficient and heat transfer rate increase with time t^* and that the effect of the time variations is found to be more pronounced on the skin friction coefficient than on the heat transfer rate, because the change in the freestream velocity with time strongly affects the velocity component.

5. Conclusions

Results indicate that the skin friction and heat transfer coefficients are significantly affected by the time-dependent freestream velocity distributions. It is found that the buoyancy force enhances the skin friction

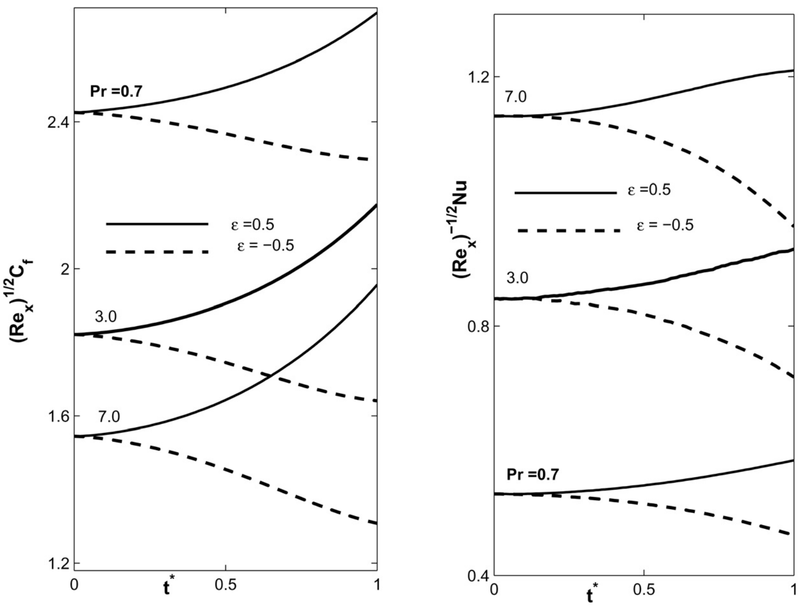

Fig. 4. Effect of Pr on $Re_x^{1/2}C_f$ and $Re_x^{-1/2}Nu$ for $\phi(t^*) = 1 + \epsilon t^2$, $\epsilon = 0.5$ and $\epsilon = -0.5$ when $\lambda = 1$, $Ec = 0.1$, $\alpha = 1$, $\xi = 0.5$.

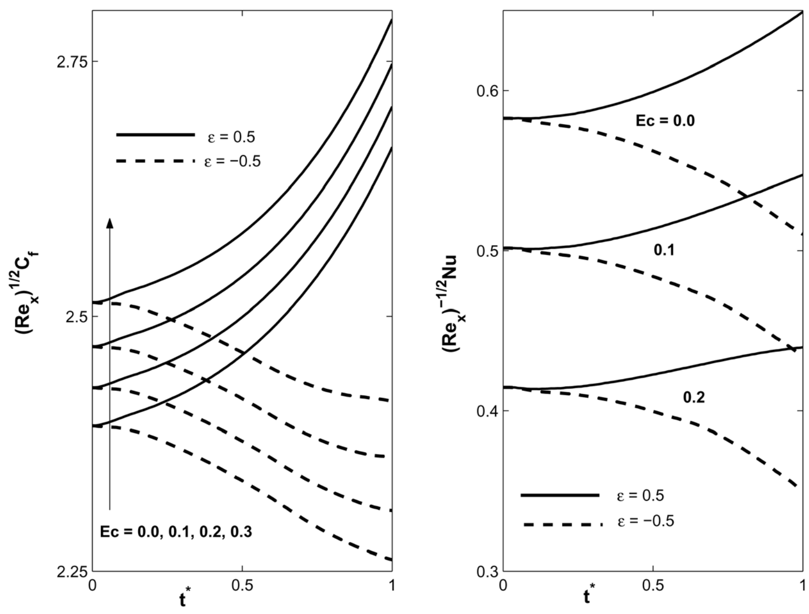

Fig. 5. Effect of Ec on $Re_x^{1/2}C_f$ and $Re_x^{-1/2}Nu$ for $\phi(t^*) = 1 + \epsilon t^{\,2}$, $\epsilon = 0.5$ and $\epsilon = -0.5$ when $\lambda = 1$, $Pr = 0.7$, $\alpha = 1$, $\xi = 0.5$.

coefficient and Nusselt number. In the presence of the buoyancy force, the velocity profile exhibits velocity overshoot for lower Prandtl numbers. Further, it is noted that the curvature parameter steepens both the velocity and temperature profiles, but injection ($A < 0$) does the reverse. The heat transfer rate is found to depend strongly on viscous dissipation, but the skin friction is little affected by it.

References

[1] Chen TS, Mucoglu A. Buoyancy effects on forced convection along a vertical cylinder. ASME J Heat Transfer 1975;97:198–203.

[2] Mucoglu A, Chen TS. Buoyancy effects on forced convection along a vertical cylinder with uniform surface heat flux. ASME J Heat Transfer 1976;98:523–525.

[3] Bui MN, Cebeci T. Combined free and forced convection on vertical slender cylinders. ASME J Heat Transfer 1985;107:476–478.

[4] Wang TY, Kleinstruver C. General analysis of steady mixed convection heat transfer on vertical slender cylinders. ASME J Heat Transfer 1989;111:393–398.

[5] Takhar HS, Chamkha AJ, Nath G. Combined heat and mass transfer along a vertical moving cylinder with a free stream. Heat Mass Transfer 2000;36:237–246.

[6] Pop I, Ingham DB. Convective Heat Transfer: Mathematical and Computational Modelling of Viscous Fluids and Porous Media. London: Pergamon, 2001.

[7] Bejan A. Convective Heat Transfer. New York: Wiley Interscience, 1994.

[8] Inouye K, Tate A. Finite difference version quasilinearization applied to boundary layer equations. AIAA J 1974,12:558–560.

[9] Varga RS. Matrix Iterative Analysis. New York: Prentice Hall, 2000.